

GeneChip, HU133A) were also determined to better define how chromosomal abnormalities influenced gene expression patterns in the affected region and to identify candidate genes that conjointly promoted increased growth rate in HL60RG cells. The DNA methylation status of two new candidate genes was assayed to elucidate the regulatory mechanisms involved in gene expression.

The results of SNP array experiments in combination with gene expression assays and DNA methylation analysis, provided insights into the mechanism of increased growth rate in HL60RG cells.

2. Material and methods

2.1. Cell lines and DNA/RNA preparation

HL60 (JCRB0085) and HL60RG (JCRB0006) cell lines were obtained from the Japanese Cancer Research Resources Bank (JCRB) and were cultured in RPMI 1640 medium supplemented with 10% heat-inactivated fetal bovine serum and kanamycin (50 µg/mL). The cultures were incubated at 37 °C in 5% atmospheric CO₂ and 100% humidity.

Total genomic DNA was extracted from cells using a DNA extractor WB Kit (Wako Pure Chemical Industries, Osaka, Japan). Total RNA was isolated and purified from cells by RNeasy columns (Qiagen, Valencia, CA). Gel electrophoresis and ethidium bromide staining were used to assess the quality of DNA and RNA preparations.

2.2. G-banding and M-FISH

Cytogenetic analysis was performed using an unstimulated suspension in RPMI 1640 medium with 15% fetal calf serum. Metaphase chromosomes were banded using a standard G-banding protocol [11,12]. For each cell line, at least 20 metaphases were analyzed. Karyotype descriptions were conformed to the ISCN [13].

M-FISH reagents were acquired from SKY Paint™ Kit (Applied Spectral Imaging, Israel). Fresh slides were prepared using standard cytogenetic protocols from archived fixed-cell material. Assays for M-FISH were performed according to the manufacturer's protocols from MetaSystems (Altlusheim, Germany). Briefly, slide and probe cocktails were denatured for 5 min at 75 °C with 70% formamide. Following a 2-day hybridization, washing and post hybridization steps were followed by the manufacturer's SKY Paint™ Kit. Slides were counterstained with DAPI. Ten metaphases were analyzed using a Zeiss microscope (Axioplan 2; Zeiss, Oberkochen, Germany) equipped with the appropriate filters (DAPI, Texas-Red, Spectra Orange, FITC, Cy5, Cy5.5) and the MetaSystems ISIS imaging software programs.

2.3. SNP 10K mapping array analysis

2.3.1. SNP chip hybridization

DNA samples were processed according to the standard GeneChip Mapping 10K (V2.0) Xba assay protocol (Affymetrix Inc., Santa Clara, CA). Reference human genomic DNA supplied in the assay kit was used as a control for the calculation of copy number changes. Briefly, 250 ng of DNA was digested with XbaI and ligated with the XbaI adaptor prior to PCR amplification (35 cycles) using AmpliTaq Gold with Buffer II (Applied Biosystems, Foster City, CA). Hybridized arrays were processed with an Affymetrix Fluidics Station 450 and fluorescence signals were detected using the Affymetrix GeneChip Scanner 3000.

2.3.2. Analysis of SNP Chip Data

Alleles (AA, AB, or BB) at each SNP were determined using the algorithm of Lin et al. [10] as implemented in the Affymetrix software package (GDAS). Regional LOH was identified whenever an uninterrupted contiguous stretch of >50 homozygous (AA or BB) genotypes was encountered with segments of DNA greater than ~15 Mb (see Section 3). Copy number changes were estimated from the allelic dosage analysis, represented by the signal intensity ratio of HL60 and HL60RG samples with the reference samples for both alleles.

2.4. Affymetrix GeneChip expression analysis

2.4.1. Chip hybridization

Samples were analyzed in duplicate and 5 µg total RNA was used as the starting material. Single cDNA synthesis, cRNA labeling, and cRNA fragmentation were conducted according to the manufacturers recommendations (Affymetrix Inc., Santa Clara, CA). The hybridization mixture was hybridized using an Affymetrix U133A human genome array. Hybridized arrays were washed and stained and fluorescence signals were detected using the Affymetrix GeneChip Scanner 3000.

2.4.2. Analysis of gene expression data

The image files were converted into expression data using the Microarray Suite Software (Affymetrix Inc., Santa Clara, CA) and the data was imported into GeneSpring software (Silicon Genetics, Redwood City, CA) for further analysis. Briefly, signal intensity was normalized by per-gene and per-chip and ratios were calculated by normalizing HL60RG samples to HL60 samples. Probe sets were filtered based on presence call. The gene selection criteria was defined as follows: for normalized data replicates that exceeded a 2-fold change in gene expression levels and reporting at least one presence call in HL60RG samples, the gene was selected as the up-regulated gene. If the normalized data replicates of HL60RG samples were lower than 0.5-fold for changes in gene expression levels, and reporting at least one presence call in the HL60 sample, the gene was selected as a down-regulated gene.

2.5. DNA methylation analysis

To determine the methylation status of *TNFRSF1B* and the *TNFRSF8* promoter, we carried out bisulfite mapping for a CpG-rich domain in the gene promoter. Bisulfite treatment of genomic DNA was performed using an EpiTect Bisulfite Kit (Qiagen, Valencia, CA) according to the manufacturer's protocol. Non CpG "C" and unmethylated CpG "C" were converted to "T", whereas methylated CpG "C" remained as "C" by the treatment.

The primers were designed (Table 1) in the region without CpG dinucleotides to amplify both methylated and unmethylated alleles. PCR products were checked by agarose gel electrophoresis. ABI PRISM BigDye Terminator Kit (PE Biosystems, USA) was used to perform direct sequencing of PCR products using an ABI PRISM 3100 genetic analyzer (Applied Biosystems Japan Ltd.).

3. Results

3.1. G-banding and M-FISH

The G-banding and M-FISH analysis were performed on the metaphase chromosome of the HL60 and HL60RG cells.

All 20 cells observed showed numerical and/or structural aberrations. The modal number was $2n = 45$ (11/20) and $2n = 46$ (9/20) for the HL60 cell, and $2n = 43$ (16/20) and $2n = 44$ (4/20) for HL60RG cell. Representative metaphases were shown in Fig. 1C and D. HL60 cell has trisomy of chromosome 6 and/or 18 and monosomy of 17 and X. Derivative chromosome of 10 and 13 were observed.

A representative image of the M-FISH analysis is shown in Fig. 1A and B. Several translocations and numerical changes were detected in both cell types, the common changes reported by Birnie [3], including deletions of the q arm of chromosome 5, were also found in both HL60 and HL60RG cells. The majority of karyotypic changes including 5p:17q translocation were detected in both cell-lines. The amplification of the *MYC* oncogene expressed on double minute chromosomes (DMs) in HL60 cells (Fig. 1A) [14] was integrated within a homogeneously staining region (HSR) on chromosome 9 in HL60RG cells (Fig. 1B). Compared with HL60 cell, the additional alteration in HL60RG is deletion in chromosome 11p, and the derivative of chromosome resulted from translocations of

Table 1

Primer design for bisulfite sequencing PCR. For primer design, get the CpG island information and DNA sequence of *TNFRSF8* and *TNFRSF1B* from the human genome browser at UCSC [41], then use a MethPrimer program to pick primer for bisulfite sequencing PCR [42].

	<i>TNFRSF1B</i> (NM.001066.2, NT.021937.19)	<i>TNFRSF8</i> (NM.001243, NT.021937.19)
Primer 5' → 3'	GGGTATTGGGGTTGAGTAG	CAAAACCTAATATTCTAAAAATC
Primer 3' → 5'	AGTGTGAATTGGAITGAGATTGTT	CCAAACCAATAACCACTTAAAAAAA
Product size	223 bp	218 bp
CpGs in product	16	14
From transcription start site	630 bp	456 bp
PCR condition	95 °C 30 s, 52 °C 30 s, 72 °C 30 s, 50 cycles	95 °C 30 s, 55 °C 30 s, 72 °C 30 s, 50 cycles

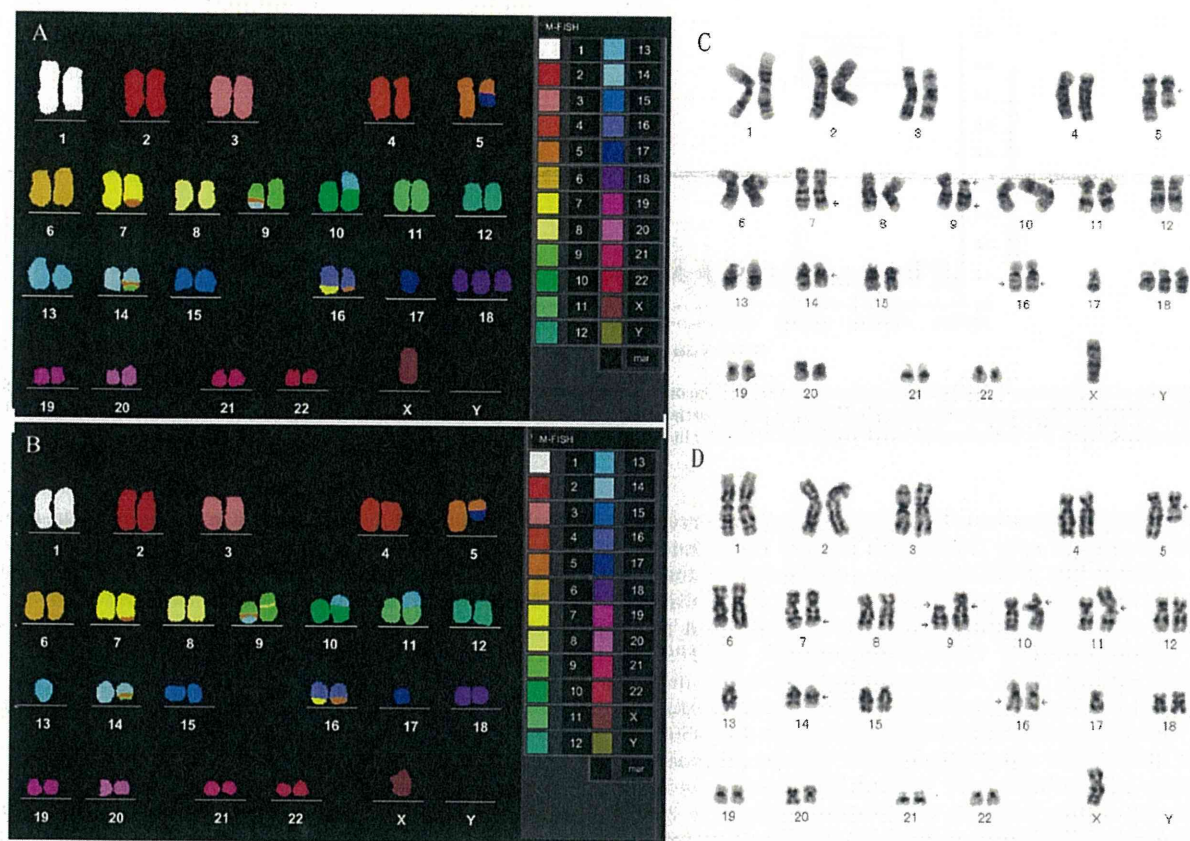


Fig. 1. Comparison of karyotypes of M-FISH and G-banding analysis in HL60 (A and C) and HL60RG (B and D). Each chromosome of M-FISH is labeled in a different color, shown in the right panel of the (A) and (B). The common changes in both cell lines are—Y, der(5)t(5;17)(q11.2;q11.2), add(7)(q32), der(9)del(9)(p13)add(9)(q37.2), add(14)(q22), add(16)(q23), -17. Compared with HL60 cell, the additional alteration in HL60RG is ins(9;7)(q13;?), der(10)t(10;13)(p11.1;q14), der(11;13)(q10;q10). The amplification of the MYC oncogene expressed on DMs in HL60 cells was integrated within a HSR on chromosome 9 in HL60RG cells.

chromosome arms 13 (Fig. 1B). The deletion in chromosome 10 occupied approximately a half of the short arm in the HL60 cells but it extended to whole 10p region in HL60RG cells. An amplification in chromosome 13q spans the shorter region in RG cells than in HL60 cell.

3.2. Genome wide analysis of LOH and copy number changes in HL60 and HL60RG cell

Allele call rates in HL60RG and HL60 samples were 98.84% and 96.76%, respectively. LOH regions were identified when segments of DNA greater than ~15 Mb and a contiguous nucleotide sequence stretch of >50 SNPs reported homozygous (AA or BB) genotypes. The characteristic chromosome alterations were observed in HL60RG but not in HL60 cells with a LOH in whole-arm chromosome 1 at 10p and 11p. Quantification of allelic copy number of the SNP call signal intensity data showed that LOH in chromosome 1 was due to UPD. This was because the copy number showed no change compared with reference human genomic DNA. However, all SNPs in chromosome 1 were homozygous genotype. The 10p and 11p LOH detected in HL60RG was caused by allelic loss/deletion. The common change in both HL60 and HL60RG cells were from hemizygous deletion at 5q, 9p, and 17p. (Table 2). Chromosomal dosage analysis showed that the region on chromosome 8q24 encompassing the MYC locus was amplified and the amplification was identified as three non-contiguous regions by SNP array in both HL60 and HL60RG cells. (Fig. 2).

Table 2
Location and type of LOH in HL60 and HL60RG cells detected by SNP 10K mapping array LOH in 5q, 9p and 17p in both cells and LOH in 11p in HL60RG were also detected by M-FISH (Fig. 1A and B).

	LOH region	LOH type
Common change in HL60 and HL60RG	5q11.2–5q31.2	Hemizygous deletion
	9p23–9p21.1	Hemizygous deletion
	17p11.2–pter	Hemizygous deletion
Detected only in HL60RG	Whole arm chromosome 1	Uniparental disomy
	10p11.21–pter	Hemizygous deletion
	11p11.2–pter	Hemizygous deletion

3.3. Gene expression analysis

To better understand how the alterations in DNA content influenced the global gene expression pattern, and to identify the candidate genes that coordinately promoted tumor progression in HL60RG, we analyzed differential gene expressions between two cells using Affymetrix U133A GeneChip. Supplemental Table 1 lists ~600 genes that significantly changed expression levels in HL60RG compared with HL60.

3.3.1. Gene expression level in chromosome 1 and differentially expressed genes TNFRSF1B and TNFRSF8

Chromosome 1 was detected to be UPD in HL60RG from SNP Chip data. A small percentage of genes showed expression level changes. The number of selected genes was less than 40 (more than 1000 genes were detected with a presence call in chromosome 1 by the array). We focused on two genes with extensive

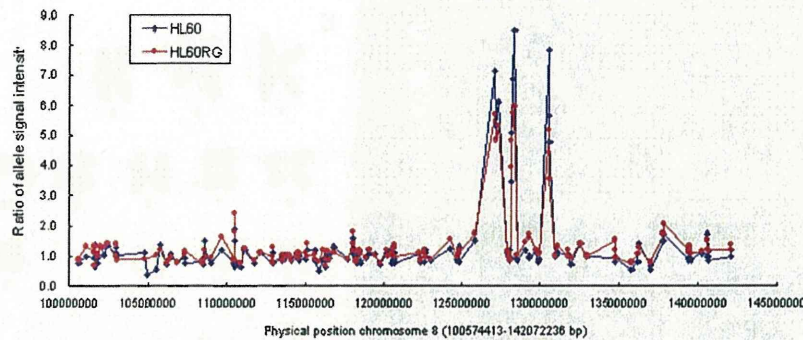


Fig. 2. Comparison of copy number plots for chromosome 8q24 of *MYC* locus between HL60 cells (blue color) and HL60RG cells (red color). The y-axis represents the probe intensity ratio of HL60/HL60RG versus reference sample. The x-axis displays the physical position on chromosome 8q24. Each '•' symbol represents a probe set from Affymetrix 10K SNP mapping array data. (For interpretation of the references to color in this figure legend, the reader is referred to the web version of this article.)

changes—*TNFRSF1B* encodes one of the tumor necrosis factor receptors and in conjunction with *TNFR1*, both mediate TNF-induced apoptosis together. The *TNFRSF8* gene is a cell surface antigen and a marker for Hodgkin lymphoma and related hematologic malignancies. Interestingly, these two genes are located adjacently in 1p36.22 (*TNFRSF8*: 12,046,021–12,126,849; *TNFRSF1B*: 12,149,647–12,191,863; UCSC Genome Browser on Human Feb. 2009 Assembly). However, the alteration was observed to be totally opposite. The expression of *TNFRSF1B* (Systematic No. 203508.at) was lost in HL60RG. The signal intensities for the two probe sets with presence calls in HL60 were 160 and 219 respectively. In HL60RG for the absence calls, the levels corresponded to 7 and 22. The expression of *TNFRSF8* (Systematic No. 206729.at) was up-regulated for about 10 times. The signal intensity for two probes in HL60 were 114 and 97, respectively and were 969 and 1112 in HL60RG cells both probes with presence calls. This result was further confirmed by quantitative RT-PCR (data was not shown here).

3.3.2. Gene expression level in 11p11.2-pter hemizygous deletion region in HL60RG cells

Gene expression levels of the deleted chromosome 11 region in HL60 and HL60RG cells were compared by scatter plots. Fig. 3 shows the expression pattern of 11p11.2-pter genes in the HL60RG sample. Most of the genes were down-regulated in this region, but three genes, namely *IFITM1* (Systematic No. 201601.x.at and 214022.s.at), *IFITM2* (Systematic No. 201315.x.at) and *IFITM3* (Systematic No. 212203.x.at) were up-regulated by a factor greater than 2-fold. The IFN-inducible transmembrane (*IFITM*) family of genes have been reported to function as a molecular marker in some tumors [15,16]. It has been demonstrated that loss of the maternal allele in 11p is involved in the pathogenesis of cancer [17,18]. In this study, maternally imprinted genes, namely *CDKN1C* (cyclin-dependent kinase inhibitor 1C, Systematic No. 213348.at), *KCNQ1* (potassium voltage-gated channel, KQT-like subfamily, member 1, Systematic No. 204486.at), and *TSSC4* (tumor-suppressing subchromosomal transferable fragment 4, Systematic No. 218671.s.at) detected by the array were down regulated. However, paternally expressed genes, *IGF2* and *INS* showed no change in expression levels in HL60RG; which suggested that the deletion event might occur in the maternal chromosome.

3.3.3. The other differentially expressed genes and *MYC* expression

Numerous changes involved in increased growth rate in HL60RG cells were detected by expression array. Expression levels of *HLA*s, *S100-A8* and 9, and *ELA2*, which was high in HL60, fell down to

the absent call in HL60RG. Inversely, a most striking up-regulation in HL60RG was observed for interleukin 32 (*IL32*, Systematic No. 203828.s.at) and hepatocyte growth factor (*HGF*, Systematic No. 209960.at, 210997.at, 210998.s.at and 210755.at), which expression was absent in HL60. The expression levels in *MYC* showed no differences among the cell lines in this study.

3.4. DNA methylation status in promoter region of *TNFRSF8* and *TNFRSF1B* genes

To study whether the opposite expression changes in *TNFRSF8* and *TNFRSF1B* were a consequence of UPD on chromosome 1, we investigated the DNA methylation status in the promoter region of both genes. The number of the CpG island in the promoter region in *TNFRSF8* and *TNFRSF1B* was 63 and 90 respectively. Primers were designed for these regions and methylation-specific PCRs were conducted (see Section 2). The sequence analysis showed *TNFRSF8* was unmethylated in HL60RG and only one allele was methylated in HL60, as shown in Fig. 4A, C peak and T peak were overlapped in HL60 compared with HL60RG, which means half of CpG "C" was

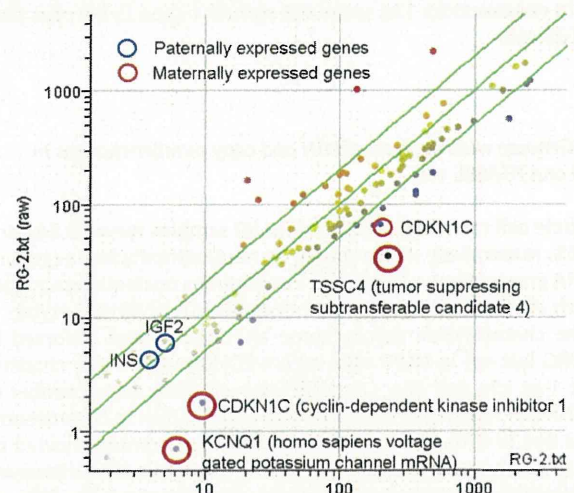


Fig. 3. Scatter plots of gene expression in LOH region (11p11.2-pter) of HL60RG. In the scatter plot view, each '•' symbol represents a gene, the vertical position of each gene represents its expression level in the HL60RG, and the horizontal position represents its control strength. Thus, genes that fall above the diagonal are overexpressed and genes that fall below the diagonal are underexpressed in the HL60RG cells. The maternally expressed genes were marked with red circles and the paternally expressed genes were marked with blue circles respectively, and the names were given. (For interpretation of the references to color in this figure legend, the reader is referred to the web version of this article.)

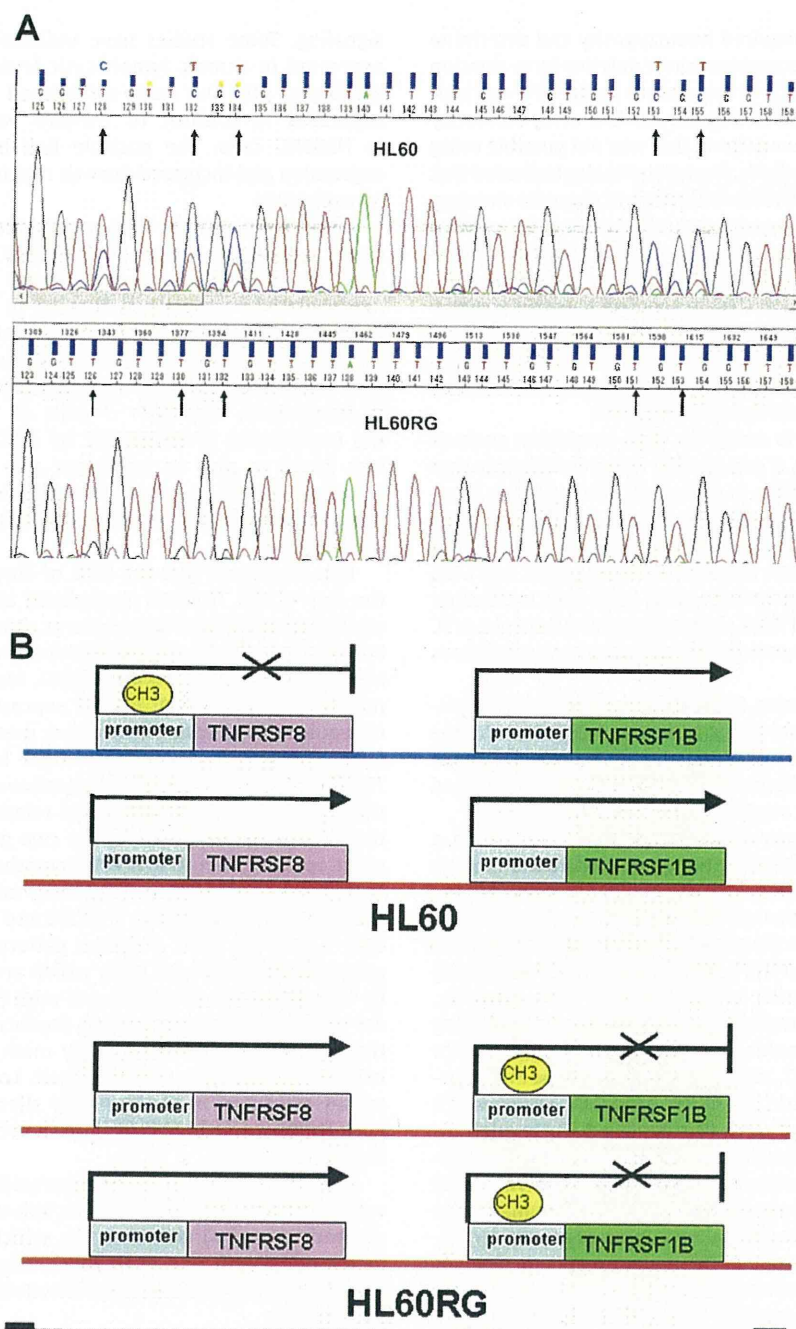


Fig. 4. (A) The DNA sequences and methylation status in *TNFRSF8* promoter region. Five CpG sites (arrow) were contained in this illustration. With the bisulfite sequencing method, "C"s in unmethylated CpG were converted into "T", whereas those in methylated CpG were kept as "C". The upper panel (HL60) showed all CpG sites contain both "C" and "T" signals, but the lower panel (HL60RG) showed all "C" at CpG sites were converted into "T". (B) The promoter methylation status and gene expression of *TNFRSF8* and *TNFRSF1B* in HL60 (upper panel) and HL60RG cells (lower panel). One horizontal line (red or blue) represents the paternal, the other represents the maternal chromosome. → represents gene expression, X represents the lost of gene expression.

converted into T by bisulfite modification, that is, one allele of *TNFRSF8* was methylated, while both parental alleles in *TNFRSF1B* were unmethylated. However, in HL60RG cells, both parental alleles were unmethylated in *TNFRSF8* but methylated in *TNFRSF1B* (Fig. 4B).

The gene expression data showed that *TNFRSF8* in HL60RG cells was over-expressed and was accompanied by the loss of methylation in the promoter region; while *TNFRSF1B* in HL60RG cells was under-expressed with both alleles methylated (Fig. 4B).

4. Discussion

HL60 has been extensively used as a model for myeloid differentiation and leukemia. HL60RG, the sub-cell-line of HL60 exhibits a higher growth rate. A comparative study on chromosomal changes in these cells would provide information about the mechanism of malignant progression. In this study, we used G-banding, M-FISH and Affymetrix 10K SNP mapping array to identify and characterize genomic alterations in HL60RG. As described previously, SNP arrays

can detect the presence of acquired homozygosity and determine whether it is due to mitotic recombination or deletion by evaluation of the signal intensity [9,10,19]. In the present study, UPD on chromosome 1 in HL60RG was detected by the 10K SNP array but not by the M-FISH and G-banding; something that was not possible using conventional cytogenetic methods. Reports have also indicated that this technology is useful for the identification of genomic changes, particularly for UPD in acute myelogenous leukemia (AML), which represents a genetically heterogeneous disease [20–22]. UPD is thought to contribute to leukemogenesis by causing homozygosity of gene mutations located in their respective genomic regions. UPD may also arise by duplication of a chromosomal segment harboring imprinted genes. UPD in chromosome 1 in HL60RG cells can lead to critical changes in gene expression that may be relevant for the issue of the increased growth rate in HL60RG.

10K SNP mapping array is useful for high-resolution analysis of chromosomal imbalances. It can identify novel imbalances that other techniques cannot resolve. In this study, the region on chromosome 8q24 encompassing the *MYC* locus was amplified as three non-contiguous regions in both HL60 and HL60RG cells. Studies using conventional cytogenetic methods including FISH and CGH had reported the major amplicon present in HL60 cells is chimeric in nature, being composed of DNA sequence derived from the *MYC* locus linked to novel DNA sequence derived from a non-contiguous region at 8q24 [23,24].

Genome-wide analysis using SNP array has verified the existence of multiple chromosomal abnormalities in HL60RG. To define how the genomic aberrations interacted with gene dosage changes that conjointly promote rapid growth in HL60RG, we determined changes in gene levels using expression array methodology.

In 11p11.2-pter hemizygous deletion region of HL60RG cells, a significant correlation was found between perturbations in gene expression and DNA content (Fig. 3). Particular genes located in the deletion region exhibited increased expression levels. These candidate genes may be involved in the progression of HL60RG. The *IFITM* family of genes that include *IFITM1*, *IFITM2* and *IFITM3* have been reported as a molecular marker in some tumors [15]. However, the decreased expression of maternally imprinted genes including *CDKN1C*, *KCNQ1*, and *TSSC4* in this region may be a causal factor for tumor progression of HL60RG, as these genes are essential for normal growth and development [25]. Other candidate genes with a significant gene dosage change were also identified. Up-regulations of *HGF* and *IL32* suggested these factors act as autocrines to stimulate the growth of HL60RG cells; *HLA* class-I was down-regulated in HL60RG cells and has been reported in a variety of malignancies and can unfavorably influence clinical outcomes, promoter hypermethylation was found to be one of the major epigenetic changes responsible for gene inactivation [26–28]. All of these genes may conjointly induce increased growth rate and malignancy development in HL60RG cells. The pathway analysis was performed on the further selected 176 genes based on the intensity dependent fold-change, using the GeneSpring (Agilent) software. This latter analysis revealed a large set of directly interacting genes (25/176), including *HGF*, *TNFRSF8*, *TNFAIP3*, *CXCR4*, *HLA*-family (A, B, C, E, and F), and S100 calcium binding proteins (A6, A8 and A9) (Supplemental Fig. 1). Gene ontology analysis resulted in a condensation of genes belonging to the category “response to external stimulus” (6–16%) (Supplemental Fig. 2).

The expression level of genes located on chromosome 1 in HL60RG did not show a distinct perturbation compared with HL60. Two genes, *TNFRSF8* and *TNFRSF1B* are both members of the TNF-receptor superfamily and were viewed as candidate genes. Both genes are reported to be associated with apoptosis, but neither has been extensively studied. *TNFRSF8* has been used as a marker of disease activity in various lymphomas [29–32]. *TNFRSF1B* has been found to be involved in both proapoptotic and antiapoptotic

signaling. Some studies have indicated that *TNFRSF1B* is over-expressed in chronic lymphocytic leukemia but not in follicular lymphoma [33]. Our study established that *TNFRSF1B* was under-expressed in contrast to *TNFRSF8* which was over-expressed in HL60RG cells. The possible link between changes in gene expression and increased growth rate in HL60RG requires further investigation.

We determined the DNA methylation status in the transcriptional regulatory region of *TNFRSF1B* and *TNFRSF8*. We found *TNFRSF8* in HL60 to be methylated on one allele and non-methylated on the other. However, in HL60RG cells both alleles were non-methylated. The aberrant methylation of the TNF(R) gene family is associated with some disease progression, overexpression of *CD70* (*TNFSF7*) by the hypomethylation of the promoter is reported in the CD4⁺ T cells of lupus patients [34], and the inactivation of *TNFRSF10C* by CpG island hypermethylation was found to play an important role in pancreatic cancer cell progression [35]. It is interesting to know whether a common mechanism exist for controlling TNF (R) gene family expression by methylation.

It is presumed that the UPD of chromosome 1 may result in the loss of the *TNFRSF8* methylated allele and may lead to up-regulation of *TNFRSF8* expression as shown in HL60RG. By contrast, both parental alleles of *TNFRSF1B* showed an unmethylated pattern in HL60 but methylated in HL60RG. Methylation of the promoter may cause the loss of *TNFRSF1B* expression. Further investigation is required to determine whether methylation of the *TNFRSF1B* gene promoter is dependent on the loss of methylation of the *TNFRSF8* gene promoter. No studies have been reported concerning the methylation mechanism and relationship between methylation and gene expression of the two genes. Based on our study, we propose for the first time a hypothesis that the expression of both genes (*TNFRSF1B* and *TNFRSF8*) may be conjointly regulated through DNA methylation. *TNFRSF8* and *TNFRSF1B* are separated by only ~23 kb on 1p36. A similar pattern was shown exist on two genes, namely *H19* and *IGF2*, which are located in close proximity both in human (11p15.5) and mice (distal chromosome 7) and are reciprocally imprinted [36]. Studies on *H19* showed the inactive paternal allele to be heavily methylated whereas the active maternal allele was unmethylated. Loss of the maternal allele causes activation of the normally silent maternal allele of *IGF2*. Both *TNFRSF8* and *TNFRSF1B* were shown to behave similarly in our study [37–40].

In brief, two types of array-generated data (SNP and expression) were collected from HL60 and its sub-cell-line HL60RG. Genomic aberrations and candidate genes, which may be associated with increased growth rate in HL60RG, were identified. These results should aid our understanding of the mechanism of tumor malignant progression.

Conflict of interest statement

The authors have no conflicts of interest to declare.

Acknowledgment

This work was supported by the Grant-in Aid for Scientific Research from the Ministry of Health, Labor, and Welfare of Japan.

Appendix A. Supplementary data

Supplementary data associated with this article can be found, in the online version, at doi:10.1016/j.mrfmmm.2011.10.005.

References

- [1] R.E. Gallagher, A.C. Ferrari, A.W. Zulich, R.W. Yen, J.R. Testa, Cytotoxic and cytodifferentiative components of 6-thioguanine resistance in HL-60 cells containing acquired double minute chromosomes, *Cancer Res.* 44 (1984) 2642–2653.
- [2] S.J. Collins, R.C. Gallo, R.E. Gallagher, Continuous growth and differentiation of human myeloid leukaemic cells in suspension culture, *Nature* 270 (1977) 347–349.
- [3] G.D. Birnie, The HL60 cell line: a model system for studying human myeloid cell differentiation, *Br. J. Cancer Suppl.* 9 (1988) 41–45.
- [4] S. Collins, M. Groudine, Amplification of endogenous myc-related DNA sequences in a human myeloid leukaemia cell line, *Nature* 298 (1982) 679–681.
- [5] R. Dalla-Favera, F. Wong-Staal, R.C. Gallo, Onc gene amplification in promyelocytic leukaemia cell line HL-60 and primary leukaemic cells of the same patient, *Nature* 299 (1982) 61–63.
- [6] D. Wolf, V. Rotter, Major deletions in the gene encoding the p53 tumor antigen cause lack of p53 expression in HL-60 cells, *Proc. Natl. Acad. Sci. U.S.A.* 82 (1985) 790–794.
- [7] S. Misawa, S.P. Staal, J.R. Testa, Amplification of the c-myc oncogene is associated with an abnormally banded region on chromosome 8 or double minute chromosomes in two HL-60 human leukemia sublines, *Cancer Genet. Cytogenet.* 28 (1987) 127–135.
- [8] Y. Honma, K. Takenaga, T. Kasukabe, M. Hozumi, Induction of differentiation of cultured human promyelocytic leukemia cells by retinoids, *Biochem. Biophys. Res. Commun.* 95 (1980) 507–512.
- [9] M.O. Hoque, C.C. Lee, P. Cairns, M. Schoenberg, D. Sidransky, Genome-wide genetic characterization of bladder cancer: a comparison of high-density single-nucleotide polymorphism arrays and PCR-based microsatellite analysis, *Cancer Res.* 63 (2003) 2216–2222.
- [10] M. Lin, L.J. Wei, W.R. Sellers, M. Lieberfarb, W.H. Wong, C. Li, dChipSNP: significance curve and clustering of SNP-array-based loss-of-heterozygosity data, *Bioinformatics* 20 (2004) 1233–1240.
- [11] M. Seabright, A rapid banding technique for human chromosomes, *Lancet* 2 (1971) 971–972.
- [12] H.C. Wang, S. Fedoroff, Banding in human chromosomes treated with trypsin, *Nat. New Biol.* 235 (1972) 52–54.
- [13] N. Standing Committee on Human Cytogenetic and M. Felix ISCN 1995: an international system for human cytogenetic nomenclature (1995): recommendations of the International Standing Committee on Human Cytogenetic Nomenclature, Memphis, Tennessee, USA, October 9–13, 1994, Karger, 1995.
- [14] P. Nowell, J. Finan, R. Dalla-Favera, R.C. Gallo, A. ar-Rushdi, H. Romanczuk, J.R. Selden, B.S. Emanuel, G. Rovera, C.M. Croce, Association of amplified oncogene c-myc with an abnormally banded chromosome 8 in a human leukaemia cell line, *Nature* 306 (1983) 494–497.
- [15] P. Andreu, S. Colnot, C. Godard, P. Laurent-Puig, D. Lamarque, A. Kahn, C. Perret, B. Romagnolo, Identification of the IFITM family as a new molecular marker in human colorectal tumors, *Cancer Res.* 66 (2006) 1949–1955.
- [16] N.T. Seyfried, L.C. Huysentruyt, J.A. Atwood 3rd., Q. Xia, T.N. Seyfried, R. Orlando, Up-regulation of NG2 proteoglycan and interferon-induced transmembrane proteins 1 and 3 in mouse astrocytoma: a membrane proteomics approach, *Cancer Lett.* 263 (2008) 243–252.
- [17] S. Albrecht, D. von Schweinitz, A. Waha, J.A. Kraus, A. von Deimling, T. Pietsch, Loss of maternal alleles on chromosome arm 11p in hepatoblastoma, *Cancer Res.* 54 (1994) 5041–5044.
- [18] S. Rainier, L.A. Johnson, C.J. Dobry, A.J. Ping, P.E. Grundy, A.P. Feinberg, Relaxation of imprinted genes in human cancer, *Nature* 362 (1993) 747–749.
- [19] R. Mei, P.C. Galipeau, C. Prass, A. Berne, G. Ghandour, N. Patil, R.K. Wolff, M.S. Chee, B.J. Reid, D.J. Lockhart, Genome-wide detection of allelic imbalance using human SNPs and high-density DNA arrays, *Genome Res.* 10 (2000) 1126–1137.
- [20] M.J. Walter, J.E. Payton, R.E. Ries, W.D. Shannon, H. Deshmukh, Y. Zhao, J. Baty, S. Heath, P. Westervelt, M.A. Watson, M.H. Tomasson, R. Nagarajan, B.P. O'Gara, C.D. Bloomfield, K. Mrozek, R.R. Selzer, T.A. Richmond, J. Kitzman, J. Geoghegan, P.S. Eis, R. Maupin, R.S. Fulton, M. McLellan, R.K. Wilson, E.R. Mardis, D.C. Link, T.A. Graubert, J.F. DiPersio, T.J. Ley, Acquired copy number alterations in adult acute myeloid leukemia genomes, *Proc. Natl. Acad. Sci. U.S.A.* 106 (2009) 12950–12955.
- [21] J. Boultonwood, J. Perry, R. Zaman, C. Fernandez-Santamaria, T. Littlewood, R. Kusec, A. Pellagatti, L. Wang, R.E. Clark, J.S. Wainscoat, High-density single nucleotide polymorphism array analysis and ASXL1 gene mutation screening in chronic myeloid leukemia during disease progression, *Leukemia* 24 (2010) 1139–1145.
- [22] L. Bullinger, J. Kronke, C. Schon, I. Radtke, K. Urbauer, U. Botzenhardt, V. Gaidzik, A. Cario, C. Senger, R.F. Schlenk, J.R. Downing, K. Holzmann, K. Dohner, H. Dohner, Identification of acquired copy number alterations and uniparental disomies in cytogenetically normal acute myeloid leukemia using high-resolution single-nucleotide polymorphism analysis, *Leukemia* 24 (2010) 438–449.
- [23] S. Feo, C. Di Liegro, R. Mangano, M. Read, M. Fried, The amplicons in HL60 cells contain novel cellular sequences linked to MYC locus DNA, *Oncogene* 13 (1996) 1521–1529.
- [24] R. Mangano, E. Piddini, L. Carramusa, T. Duhig, S. Feo, M. Fried, Chimeric amplicons containing the c-myc gene in HL60 cells, *Oncogene* 17 (1998) 2771–2777.
- [25] S.M. Tilghman, The sins of the fathers and mothers: genomic imprinting in mammalian development, *Cell* 96 (1999) 185–193.
- [26] A.G. Menon, H. Morreau, R.A. Tollenaar, E. Alphenaar, M. Van Puijenbroek, H. Putter, C.M. Janssen-Van Rhijn, C.J. Van De Velde, G.J. Fleuren, P.J. Kuppen, Down-regulation of HLA-A expression correlates with a better prognosis in colorectal cancer patients, *Lab. Invest.* 82 (2002) 1725–1733.
- [27] E.C. Castelli, C.T. Mendes-Junior, J.L. Viana de Camargo, E.A. Donadi, HLA-G polymorphism and transitional cell carcinoma of the bladder in a Brazilian population, *Tissue Antigens* 72 (2008) 149–157.
- [28] Q. Ye, Y. Shen, X. Wang, J. Yang, F. Miao, C. Shen, J. Zhang, Hypermethylation of HLA class I gene is associated with HLA class I down-regulation in human gastric cancer, *Tissue Antigens* 75 (2010) 30–39.
- [29] A. Caleo, A. Sanchez-Aguilera, S. Rodriguez, A.M. Dotor, L. Beltran, A.F. de Larriño, F.J. Menarguez, M.A. Piris, J.F. Garcia, Composite Hodgkin lymphoma and mantle cell lymphoma: two clonally unrelated tumors, *Am. J. Surg. Pathol.* 27 (2003) 1577–1580.
- [30] M.Z. Dewan, M. Watanabe, S. Ahmed, K. Terashima, S. Horiuchi, T. Sata, M. Honda, M. Ito, T. Watanabe, R. Horie, N. Yamamoto, Hodgkin's lymphoma cells are efficiently engrafted and tumor marker CD30 is expressed with constitutive nuclear factor-kappaB activity in unconditioned NOD/SCID/gammac (null) mice, *Cancer Sci.* 96 (2005) 466–473.
- [31] S.H. Nam-Cha, S. Montes-Moreno, M.T. Salcedo, J. Sanjuan, J.F. Garcia, M.A. Piris, Lymphocyte-rich classical Hodgkin's lymphoma: distinctive tumor and microenvironment markers, *Mod. Pathol.* (2009).
- [32] P. Valent, K. Sotlar, H.P. Horny, Aberrant expression of CD30 in aggressive systemic mastocytosis and mast cell leukemia: a differential diagnosis to consider in aggressive hematopoietic CD30-positive neoplasms, *Leuk. Lymphoma* 52 (2011) 740–744.
- [33] D. Hui, N. Satkunam, M. Al Kaptan, T. Reiman, R. Lai, Pathway-specific apoptotic gene expression profiling in chronic lymphocytic leukemia and follicular lymphoma, *Mod. Pathol.* 19 (2006) 1192–1202.
- [34] Y. Luo, M. Zhao, Q. Lu, Demethylation of promoter regulatory elements contributes to CD70 overexpression in CD4+ T cells from patients with subacute cutaneous lupus erythematosus, *Clin. Exp. Dermatol.* 35 (2010) 425–430.
- [35] H.H. Cai, Y.M. Sun, Y. Miao, W.T. Gao, Q. Peng, J. Yao, H.L. Zhao, Aberrant methylation frequency of TNFRSF10C promoter in pancreatic cancer cell lines, *Hepatobiliary Pancreat. Dis. Int.* 10 (2011) 95–100.
- [36] H. Sasaki, K. Ishihara, R. Kato, Mechanisms of Igf2/H19 imprinting: DNA methylation, chromatin and long-distance gene regulation, *J. Biochem.* 127 (2000) 711–715.
- [37] S. Zemel, M.S. Bartolomei, S.M. Tilghman, Physical linkage of two mammalian imprinted genes, H19 and insulin-like growth factor 2, *Nat. Genet.* 2 (1992) 61–65.
- [38] W. Reik, A. Murrell, Genomic imprinting. Silence across the border, *Nature* 405 (2000) 408–409.
- [39] S. Kurukuti, V.K. Tiwari, G. Tavoosidana, E. Pugacheva, A. Murrell, Z. Zhao, V. Lobanenkov, W. Reik, R. Ohlsson, CTCF binding at the H19 imprinting control region mediates maternally inherited higher-order chromatin conformation to restrict enhancer access to Igf2, *Proc. Natl. Acad. Sci. U.S.A.* 103 (2006) 10684–10689.
- [40] I.A. De La Rosa-Velazquez, H. Rincon-Arango, L. Benitez-Briebesca, F. Recillas-Targa, Epigenetic regulation of the human retinoblastoma tumor suppressor gene promoter by CTCF, *Cancer Res.* 67 (2007) 2577–2585.
- [41] W.J. Kent, C.W. Sugnet, T.S. Furey, K.M. Roskin, T.H. Pringle, A.M. Zahler, D. Haussler, The human genome browser at UCSC, *Genome Res.* 12 (2002) 996–1006.
- [42] L.C. Li, R. Dahiya, MethPrimer: designing primers for methylation PCRs, *Bioinformatics* 18 (2002) 1427–1431.

Detection of Genotoxicity of Phenolic Antioxidants, Butylated hydroxyanisole and *tert*-Butylhydroquinone in Multiple Mouse Organs by the Alkaline Comet AssayRamadan, A.M. Ali^{1,2} and Takayoshi Suzuki³¹Zoology Dept., College for Girls for Science, Arts and Education, Ain-Shams Univ., Heliopolis, Cairo, Egypt.²Division of Genetics and Mutagenesis, ³Division of Cellular and Gene Therapy Products, National Institute of Health Sciences, 1-18-1, Kamiyoga, Setagaya-ku, Tokyo 158, Japan.ramadanali27@gmail.com

Abstract: In this study we tested the genotoxicity of two widely used phenolic antioxidants, butylated hydroxyanisole (BHA) and *tert*-butylhydroquinone (TBHQ) in multiple mouse organs using the alkaline comet assay. Tissue samples from four organs (stomach, liver, kidney and bone marrow) were collected from male mice at 3 and 24 h post treatment with BHA (800 mg/kg) or TBHQ (400 mg/kg) and examined for genotoxicity. The two compounds induced significant increase in DNA migration in a time dependant manner in specific organs. Extensive DNA damage was observed in stomach cells at 24 h post treatment in treatment groups. In addition to stomach, TBHQ treatment induced significant increase in DNA migration in liver and kidney cells. Although increased DNA damage was found in kidney cells of treatment groups at 3 h time point, at later time point it was persistent only in mice treated with TBHQ and in other treatment group (BHA) it appeared to be recovered with time. Evidently, bone marrow cells did not show genotoxicity in response to treatment with TBHQ and BHA. Considering these findings, although TBHQ and BHA are generally considered non-genotoxic, the DNA damage observed in this experiment may be related to their indirect action on DNA via ROS mechanism. Since toxicity of these compounds are often ascribed to their metabolic products such as quinone thioethers and hence differences in the metabolism of these compounds may play an important role in determining the target organ of toxicity. The present work draws our attention to revising the genotoxicity of the widely used antioxidants and accepted as safe artificial antioxidants.

[Ramadan, A.M. Ali and Takayoshi Suzuki. **Detection of Genotoxicity of Phenolic Antioxidants, Butylated hydroxyanisole and *tert*-butylhydroquinone in Multiple Mouse Organs by the Alkaline Comet Assay.** Journal of American Science 2012;8(1):722-727] (ISSN: 1545-1003). <http://www.americanscience.org>. 98

Key words: BHA; TBHQ; comet assay; mice; bone marrow; liver; kidney; stomach; ENU.

1. Introduction

Butylated hydroxyanisole (BHA, 3-*tert*-butyl 4-hydroxyanisole) and its *O*-demethylated metabolite *tert*-butylhydroquinone (TBHQ) are synthetic phenolic food antioxidants widely used to protect oils, fats and shortenings from oxidative deterioration and rancidity (Finley *et al.*, 2011). Both compounds are generally non-mutagenic and nearly all short-term genotoxicity tests including the classic *Salmonella typhimurium* with or without S9 fraction (Matsuoka *et al.*, 1990), unscheduled DNA synthesis assay using rat hepatocytes, and except both positive and negative results with and without activation respectively in Chinese hamster cells for chromosomal aberration and sister chromatid exchange are negative (Matsuoka *et al.*, 1990; Williams *et al.*, 1990). On the other hand; chronic dietary administration of BHA resulted in DNA damage in forestomach of rats (Morimoto *et al.*, 1991) and papilloma and carcinoma formation in the forestomach of rats, mice and hamsters (Clayson *et al.*, 1990; Chandra *et al.*, 2010). In fact, both BHA and TBHQ have shown to contain both carcinogenic and anticarcinogenic properties (Kahl, 1997; Gharavi *et al.*, 2007). Anticarcinogenic activity of

BHA has been ascribed to its ability to induce Phase II metabolic enzymes and its free radical trapping activity (Kadoma *et al.*, 2008; Cemeli and Anderson, 2011); its carcinogenicity has been often linked to its quinone-forming metabolites, a property that BHA shares with benzene. Quinones are highly reactive molecules, which can bind to biological macromolecules (Tu *et al.*, 2011) and induce chromosomal loss or chromosomal breakage (Jacobus *et al.*, 2008).

The scope of this research is to determine the *in vivo* genotoxic effects of TBHQ and BHA in different organs of mouse. Through conducting the single cell gel electrophoresis assay (Comet assay) on four organs (stomach, liver, kidney and bone marrow) of mice treated with TBHQ (400 mg/kg) or BHA (800 mg/kg). In addition, to identify possible time dependent effect, tissue samples were collected on two occasions, 3 and 24 h post treatment and subjected to the alkaline version of the comet assay. The comet assay is a sensitive cytogenetic assay with advantages of detecting broad spectrum of DNA damages which may lead into DNA strand breaks, the need of small number of cells per sample, and the short time needed to do a complete study (Tice *et al.*,

2000). This assay could be applied to any tissue in the given *in vivo* model, and has potential advantages over other *in vivo* genotoxicity tests methods, which are reliably applicable to one or few tissues which is considered a very important matter for investigation of suspected tissue specific-genotoxic activity, which include 'site of contact' genotoxicity.

2- Material and Methods

Chemicals

All chemicals used in this study were purchased from Wako Pure Chemical Industries, Ltd. (Osaka, Japan).

Animals and treatments.

Twenty male ddY mice were obtained from Japan SLC (Shizuoka, Japan) at 7 weeks of age and used after one week of acclimatization. They were maintained at 20 -24°C and 55-65 % humidity with a 12-hr light-dark cycle and fed commercial pellets (Oriental Yeast Industries Co., Tokyo, Japan) and tap water *ad libitum*. Aqueous solutions of TBHQ (400 mg/kg) and BHA (800 mg/kg) were administered intragastrically to two groups of three mice at a dose level of 10 ml/kg. A positive control (ENU, 20 mg/kg) group of two mice were treated at the same time in the same manner. The animals were sacrificed by cervical dislocation at 3 h and 24 h after treatment and four organs - bone marrow, liver, kidney and stomach - were dissected out. Tissue samples were collected from four untreated mice at the latter sampling point (24 h) and treated as the negative control.

The tissue samples except bone marrow were washed in saline, minced, suspended at a concentration of 1 g/ml in ice cold homogenizing buffer (HBSS with 20 mM EDTA, 10% DMSO, pH 7.5) and homogenized gently using a Dounce's homogenizer. The marrow was collected from the femur bones and suspended in 1 ml of chilled homogenizing buffer. The cell suspensions were diluted in chilled homogenizing buffer appropriately and subjected to the alkaline comet assay immediately (Tice *et al.*, 2000).

Comet assay

The alkaline comet assay was performed basically as described by Miyamae *et al.* (1998) with few modifications. The cell suspensions prepared as above were mixed 1: 1 (v/v) with 1% low melting point (37°C) agarose (LMA) prepared in PBS, pH 7.4 and 75 µl of the mixture was quickly layered on a 1% normal melting point agarose (NMA) (prepared in distilled water) precoated and overnight dried slides and covered with a coverslip. Then the slides were placed on a chilled plate to allow complete

polymerization of agarose. Finally 75 µl of 0.5% NMA in PBS was quickly layered in the same manner after removing the coverslip and allowed to solidify on chilled plate. The slides were immersed in freshly made chilled lysis solution (2.5M NaCl, 100mM Na₂EDTA, 10mM Trizma base, 10% DMSO and 1% Triton X-100; pH 10.0) in dark at 4°C for 60 min. The slides were then placed in a horizontal electrophoresis tank containing electrophoresis buffer (300mM NaOH and 1mM Na₂EDTA; pH 13.0) for 10 min, allowing salt equilibration and further DNA unwinding before electrophoresis at 25 V (0.8V/cm), 300 mA for 20 min. The slides were washed three times (5 min each) with chilled neutralizing buffer, 0.4M Tris-HCl (pH 7.5). After the third wash, the slides were stained with 50 µl EtBr (20 µl/ml) and covered with a coverslip. To prevent drying, the slides were stored in a humidified container until microscopic examination.

The slides were examined at 200x magnification using Olympus fluorescent microscope. All slides were coded and examined blindly. A total of 1000 randomly selected cells from two replicate slides (500 cells per slide) were examined per sample. The comets were classified into five categories (Type1 – Type 5) depending on the fraction of DNA migrated out into the tail, and thus increasing degrees of damage (Miyamae *et al.*, 1998). The comets were assigned a value of 0, 1, 2, 3 or 4 (from undamaged, 0, to maximally damaged, 4). Thus, the total score for 1000 comets ranged from 0 (all undamaged) to 4000 (all damaged) in arbitrary units (Visvardis *et al.*, 1997; Piperakis *et al.*, 1998). In this method a large number of cells can be examined in a short time.

Statistical analysis

Results of the different treatment groups were compared to data obtained from four untreated mice using Students' one-tailed *t*-test (Fowler *et al.*, 1998). Significance was indicated by *P* values <0.05

3. Results

As shown in table 1; the comet data measured by visual scoring from four organs (bone marrow, liver, kidney and stomach) from mice intragastrically treated with TBHQ (400mg/kg b.w.) or BHA (800 mg/kg b.w.) for 3 and 24 hr. In this experiment comet data obtained from four untreated mice were treated as the negative control and used for comparison. Among TBHQ treated animals, 24 hr after exposure mean DNA migration score was significantly (*P*<0.05) high in 3 organs (stomach, liver and kidney), although at earlier time point relative to control value it was different significantly only in kidney. In bone marrow the induced DNA strand breaks were not significant at both time points.

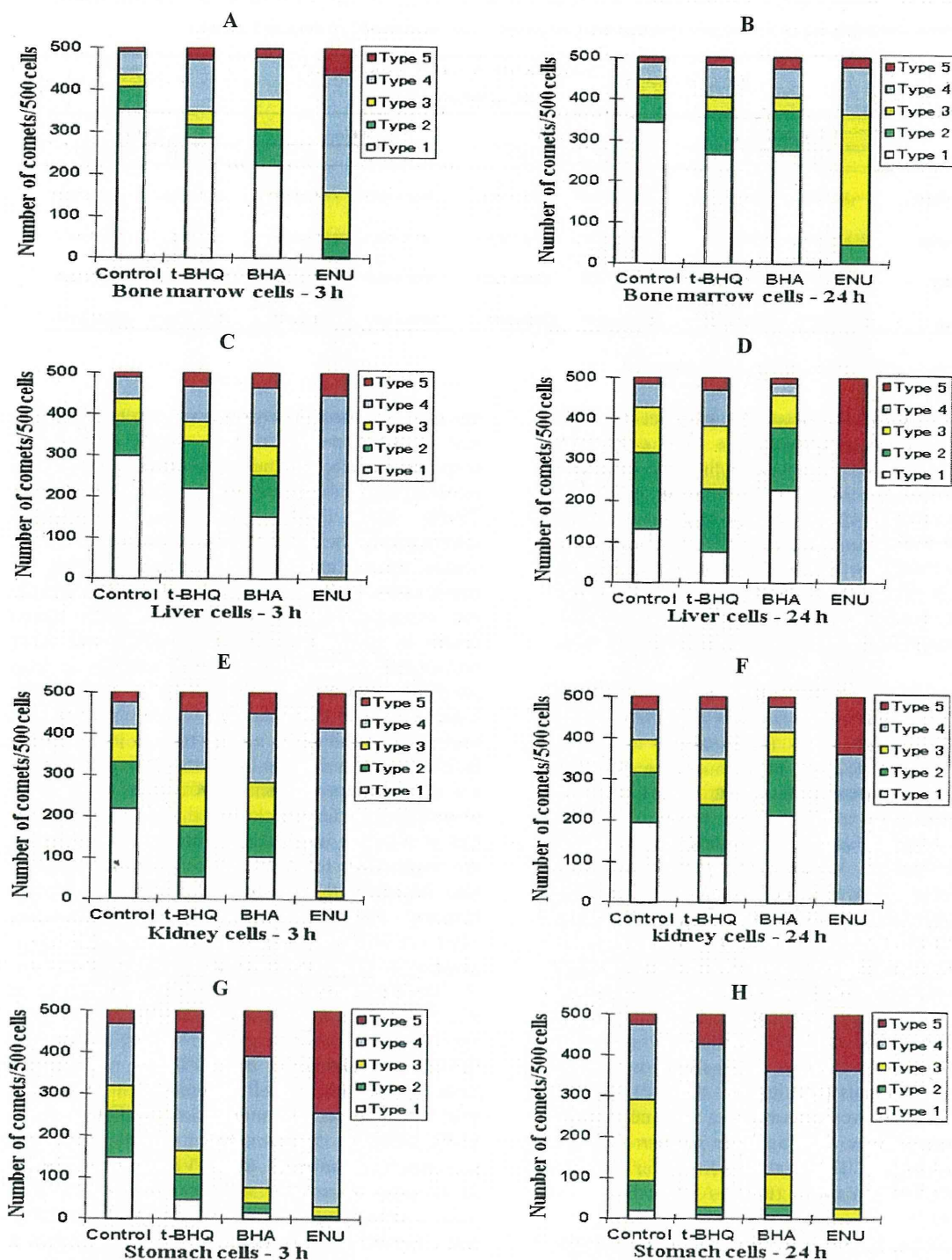


Fig. 1. Incidences of comet cells in mice treated with TBHQ (400 mg/kg b.w.), BHA (800 mg/kg b.w.) and the positive control ENU (20 mg/kg b.w.) for 3 and 24 h. The comet cells derived from bone marrow (Figs. 1A and 1B), liver (Figs. 1C and 1D), kidney (Figs. 1E and 1F) and stomach (Figs. 1G and 1H).

Table 1. Incidences of comet cells without type 1 in bone marrow, liver, kidney and stomach of mice treated with t-BHQ and BHA for 3 and 24 h.

Treatment	Pooled calculations of incidences of comets without type 0 (Average/500 cells \pm S.D.)							
	Bone marrow		Liver		Kidney		Stomach	
	3 h	24 h	3 h	24 h	3 h	24 h	2h	24 h
Control (Dis. H ₂ O)	146.3 \pm 125.3	156.5 \pm 16.3	202.0 \pm 116.0	369.5 \pm 99.3	283.3 \pm 110.3	305.3 \pm 94.6	350.0 \pm 109.4	479.5 \pm 14.5
t-BHQ (400 mg/kg)	213.7 \pm 136	234.3 \pm 37.7	274.5 \pm 61.3	425.2 \pm 59.6*	447.5 \pm 66.1	385.2 \pm 66.1*	453.5 \pm 29.1	490.3 \pm 8.1*
BHA (800 mg/kg)	279.3 \pm 171.5	226.0 \pm 45.1	345.0 \pm 40.5	237.2 \pm 72.2	397.2 \pm 79.1*	287.3 \pm 97.7	483.3 \pm 13.6*	490.1 \pm 11.6*
ENU (20 mg/kg)	495.0 \pm 6.0**	498.5 \pm 3.0**	500.0 \pm 0.0**	500.0 \pm 0.0***	500.0 \pm 0.0**	500.0 \pm 0.0***	498.25 \pm 2.1**	500.0 \pm 0.0***

n.b.

ns = non significant; * = (P < 0.05); * = (P < 0.01); * = (P < 0.001)

Exposure to BHA resulted in significant (P<0.05) increase in DNA migration in a time dependent manner in specific organs which was observed among stomach tissues at both sampling points, in kidney it occurred only at 3 hr time point and then decreased with time. Following BHA treatment liver and bone marrow cells did not yield any significant increase in mean DNA migration. ENU (20 mg/kg) treatment produced highly significant (P<0.001) DNA damage in all four tested organs at both time points.

Figure 1 shows the distribution pattern of nuclear DNA expressed as the percent cells in the five comet classes from Type 1 (undamaged) to Type 5 (maximally damaged) in various organs of mice belonged to different treatment groups. Except in ENU (positive control) treated group, in other samples some cells/nuclei remained undamaged (category Type 1). At both sampling time points in all treatment groups' greater numbers of comets showed high levels of DNA damage (category Type 4) in stomach cells. The frequency distribution of DNA damage among individual hepatocytes showed that the number of damaged cells and the extent of damage were greatest among mice treated with TBHQ (Figures 1-C and 1-D). Similarly in renal cells the extent of DNA damage decreased with time in BHA treated animals (Figures 1-E and 1-F). Higher levels of damage were observed in renal cells from TBHQ treated mice. Among bone marrow cells in treatment groups (TBHQ and BHA) over 50% of the cells showed no damage (Figures 1-A and 1-B)

4. Discussion

Considering the strong correlation between organ specific genotoxicity and organ specific carcinogenicity, the assessment of genotoxicity in multiple organs *in vivo* may indicate that it would be the target organ(s) in humans and provide useful information for the evaluation of chemical safety. While other *in vivo* genotoxicity tests are limited to

one or few tissues, the comet assay can be applied to any tissue provided that a single cell/nucleus suspension can be obtained. Therefore, in the present research, to test the tissue specific genotoxic effect of TBHQ and, BHA mice were administered intragastrically with the test compounds and various organs were examined for genotoxicity using the comet assay. Results of this research suggest that the test compounds induced significant DNA strand breaks in stomach cells and the effect was more pronounced among BHA treated animals at both sampling occasions. With TBHQ, a significantly higher degree of DNA damage was observed at 24 h time point, although at earlier time point (3 h) the induced DNA damage in these treatment groups were not significantly different from control data. These observations again acknowledge the earlier findings that stomach in particular forestomach in rodent is the target organ for BHA induced genotoxicity. It is also important to remember that there are several bioassay reports describing neoplasm-promoting effects of BHA and TBHQ in the fore stomach when given after initiating carcinogens such as N-methyl-N-nitro-N-nitrosoguanidine (MNNG) (Kuroiwa *et al.*, 2007; Liu and Russell, 2008), N-methyl-N-nitrosourea (NMU) and N,N-dibutyl nitrosamine (DBN) (Fukushima *et al.*, 1987). In this respect, there are studies, which demonstrated that BHA inhibits cell-to-cell communication (Williams *et al.*, 1990), which is often considered a marker for tumor promoters (Leithe *et al.*, 2006; Vinken *et al.*, 2009). In the bone marrow cells, although at earlier time point a non-significant increase in DNA migration was observed in BHA and t-BHQ treated animals, it was not persistent at latter time point and appeared to be recovered with time. *In vivo* BHA is metabolized to t-BHQ in the liver (Peters *et al.*, 1996; Moridani *et al.*, 2002). TBHQ and HQ are further oxidized to their respective quinone species, 1,4-benzoquinone and tertiary-butylquinone, which in turn may enter

into a redox cycling between quinone and hydroquinone via semiquinone radicals and can generate reactive oxygen species (Peters *et al.*, 1996; Li *et al.*, 2002). These ROS may then react with cellular protein and DNA and thus cause large-scale chromosomal alterations (Cerutti, 1985). The test compounds used in this study have been reported to be nephrotoxic and can induce tumor in rodent kidney (Shibata *et al.*, 1991; Kari *et al.*, 1992). Nonetheless, the evidence for genotoxicity as increased level of DNA migration in the liver and kidney was observed only in mice treated with t-BHQ. The nephrotoxicity of these compounds are often linked to their quinone thioether metabolites (Monks *et al.*, 1992) and their ability to react with DNA either directly (Jacobus *et al.*, 2008) or indirectly via reactive oxygen generation (Li *et al.*, 2002; Li *et al.*, 2007). Hence, differences in metabolism of these compounds and ability of their metabolites to generate ROS could be a possible reason for the observed differences in toxicity (Kadoma *et al.*, 2008).

DNA strand breaks are associated both to the removal of DNA adducts by endonuclease and to the direct action of the chemicals and/or the free radicals produced during their metabolism, which then creates both single- and double-strand breaks in DNA (Bohr, 1991). Investigations of BHA and its metabolites have not demonstrated DNA adducts formation, as measured by the sensitive [³²P] postlabelling assay (Saito *et al.*, 1989). Previous research has showed that enzymatic oxidation of TBHQ in rodent forestomach may occur via prostaglandin H synthase PHS (Schilderman *et al.*, 1993) or possibly a gastric peroxidase (Banerjee, 1988). It is widely believed that TBHQ; an *O*-demethylated metabolite of BHA probably produces many of the toxic effects ascribed to BHA. It is also postulated that BHA and TBHQ act through ROS induced oxidative damage including DNA damage (Iverson, 1995). Supporting this suggestion studies have demonstrated the formation of 8-hydroxydeoxyguanosine, a marker for reactive oxygen formation and for DNA strand breaks (Schilderman *et al.*, 1995; Okubo *et al.*, 1997), in calf thymus DNA (Nagai *et al.*, 1996) and in isolated DNA and cultured rat hepatocytes (Li *et al.*, 2002) treated with TBHQ. Peters *et al.* (1996) have demonstrated that TBHQ and its glutathione conjugates are capable of catalyzing 8-hydroxydeoxyguanosine formation and thus induce oxidative DNA damage. Further, Dobo and Eastmond (1994) have demonstrated the role of reactive oxygen species in the chromosomal breakage induced by TBHQ in a prostaglandin H synthase containing Chinese hamster V79 cell line. Considering these findings, although TBHQ and

BHA are generally considered non-genotoxic, the DNA damage observed in this experiment may be related to their indirect action on DNA via ROS mechanism. Since toxicity of these compounds are often ascribed to their metabolic products such as quinone thioethers and hence differences in the metabolism of these compounds may play an important role in determining the target organ of toxicity.

Corresponding author

Ramadan A. M. Ali

Zoology Dept., College for Girls for Science, Arts and Education, Ain-Shams Univ., Heliopolis, Cairo, Egypt. ramadanali27@gmail.com

References

1. Banerjee K. (1988). Membrane peroxidase. *Mol. Cell Biochem.*, 83: 105-128.
2. Bohr A. (1991). Gene specific DNA repair. *Carcinogenesis*, 12: 1983-1992.
3. Cemeli E. and Anderson D. (2011). Mechanistic investigation of ROS-induced DNA damage by oestrogenic compounds in lymphocytes and sperm using the comet assay. *Int. J. Mol. Sci.*, 12: 2783-2796.
4. Cerutti P. (1985). Prooxidant state and tumor promotion. *Science*, 227: 375-381.
5. Chandra S., Nolan M. and Malarkey D. (2010). Chemical carcinogenesis of the gastrointestinal tract in rodents: An overview with emphasis on NTP carcinogenesis. *Bioassays Toxicol. Pathol.*, 38: 188-197.
6. Clayson D., Iverson F., Nera E. and Lok E. (1990). The significance of induced forestomach tumors. *Ann. Rev. Pharmacol. Toxicol.*, 30:441-463.
7. Dobo L. and Eastmond A. (1994). Role of oxygen radicals in the chromosomal loss and breakage induced by the quinone-forming compounds, hydroquinone and *tert*-butylhydroquinone. *Environ. Mol. Mutagen.*, 24: 293-300.
8. Finley J., Kong A., Hintze K., Jeffery E., Ji L. and Lei X. (2011). Antioxidants in foods: state of the science important to the food industry. *J. Agric. Food Chem.*, 59 (13): 6837-6846.
9. Fowler J., Cohen L. and Jarvis P. (1998). Practical statistics for field biology. 2nd ed. John Wiley & Sons, Chichester, New York
10. Fukushima S., Ogiso T., Kurata Y., Hirose M. and Ito N. (1987). Dose-dependent effects of butylated hydroxytoluene and ethoxyquin for promotion of bladder carcinogenesis in N-butyl-N-(4-hydroxybutyl) nitrosamine-initiated, unilaterally ureter ligated rats. *Cancer Lett.*, 34: 83-90.
11. Gharavi N., Haggarty S. and El-Kadi A. (2007). Chemoprotective and carcinogenic effects of *tert*-butylhydroquinone and its metabolites. *Current Drug Metabolism*, 8: 1-7.
12. Iverson F. (1995). Phenolic antioxidants: health protection branch studies on butylated hydroxyanisole. *Cancer Lett.*, 93: 49-54.
13. Jacobus J., Flor S., Klingelhut A., Robertson L. and Ludewig G. (2008). 2-(4'-chlorophenyl)-1,4-benzoquinone increases the frequency of micronuclei

- and shortens telomeres. *Environ. Toxicol. Pharmacol.*, 25(2): 267-272.
14. Kadoma Y., Ito S., Yokoe I. and Fujisawa S. (2008). Comparative study of the alkyl and peroxy radical-scavenging activity of 2-*t*-butyl-4-methoxyphenol and its dimer, and their theoretical parameters. *In vivo*, 22: 289-296.
 15. Kahl R. (1997). Synthetic antioxidants: biochemical actions and interferences with radiation and toxic compounds, chemical mutagens and chemical carcinogens. *Toxicology*, 33: 185-228.
 16. Kari F.W., Bucher J., Eustis S.L., Haseman J.K. and Huff J.E. (1992). Toxicity and carcinogenicity of hydroquinone in F344/N rats and B6C3F₁ mice. *Food Chem. Toxicol.*, 30: 737-747.
 17. Kuroiwa Y., Ishii Y., Umemura T., Kanki K., Mitsumori K., Nishikawa A., Nakazawa H. and Hirose M. (2007). Combined treatment with green tea catechins and sodium nitrite selectively promotes rat forestomach carcinogenesis after initiation with *N*-methyl-*N'*-nitro-*N*-nitrosoguanidine. *Cancer Science*, 98: 949-957.
 18. Leithe E., Sirnes S., Omori Y. and Rivedal E. (2006). Downregulation of gap junctions in cancer cells. *Crit. Rev. Oncog.*, 12(3-4): 225-256.
 19. Li Y., Zhong F., Wu S. and Shi N. (2007). NF-E2 related factor 2 activation and heme oxygenase-1 induction by tert-butylhydroquinone protect against deltamethrin-mediated oxidative stress in PC12 cells. *Chem. Res. Toxicol.*, 20(9): 1242-51.
 20. Li Y., Seacat A., Kuppusamy P., Zweier L., Yager D. and Trush, A. (2002). Copper redox-dependent activation of 2-*tert*-butyl(1,4)hydroquinone: formation of reactive oxygen species and induction of oxidative DNA damage in isolated DNA and cultured rat hepatocytes. *Mutat. Res.*, 518: 123-133.
 21. Liu C. and Russell R. M. (2008). Nutrition and gastric cancer risk: an update. *Nutr. Rev.*, 66: 237-249.
 22. Matsuoka A., Matsui M., Miyata N., Sofuni T. and Ishidate M. Jr. (1990). Mutagenicity of 3-*tert*-butyl-4-hydroxyanisole (BHA) and its metabolites in short-term tests in vitro. *Mutat. Res.*, 241(2):125-132.
 23. Miyamae Y., Yamamoto M., Sasaki Y.F., Kobayashi H., Igarashi-Soga M., Shimoi K. and Hayashi M. (1998). Evaluation of a tissue homogenization technique that isolates nuclei for the in vivo single cell gel electrophoresis (comet) assay: a collaborative study by five laboratories. *Mutat. Res.*, 418: 131-140.
 24. Monks T.J., Hanzlik R.P., Cohen G.M., Ross D. and Graham D.G. (1992). Quinone chemistry and toxicity. *Toxicol. App. Pharmacol.*, 112: 2-16.
 25. Moridani M., Cheon S., Khan S. and O'Brien J. (2002). Metabolic activation of 4-hydroxyanisole by isolated rat hepatocytes. *Drug Metab. Dispos.*, 30(10): 1063-1069.
 26. Morimoto K., Tsuji K., Iio T., Miyata N., Uchida A., Osawa R., Kitsutaka H. and Takahashi A. (1991). DNA damage in forestomach epithelium from male F344 rats following oral administration of tert-butylquinone, one of the forestomach metabolites of 3-BHA. *Carcinogenesis*, 12(4):703-8.
 27. Nagai F., Okubo T., Ushiyama K., Satoh K. and Kano I. (1996). Formation of 8-hydroxydeoxyguanosine in calf thymus DNA treated with tert-butylhydroquinone, a major metabolite of butylated hydroxyanisole. *Toxicol. Lett.*, 89: 163-167.
 28. Okubo T., Nagai F., Ushiyama K. and Kano I. (1997). Contribution of oxygen radicals to DNA cleavage by quinone compounds derived from phenolic antioxidants, tert-butylhydroquinone and 2,5-di-*tert*-butylhydroquinone. *Toxicol. Lett.*, 90: 11-18.
 29. Peters M., Lau S., Dulik D., Murphy D., Ommen B., Bladeren P. and Monks T. (1996). Metabolism of tert-butylhydroquinone to *S*-substituted conjugates in the male Fischer 344 rat. *Chem. Res. Toxicol.*, 9: 133-139.
 30. Piperakis S.M., Visvardis E-E., Sagnou M. and Tassiou A.M. (1998). Effects of smoking and ageing on oxidative DNA damage of human lymphocytes. *Carcinogenesis*, 19: 695-698.
 31. Saito K., Nakagawa S., Yoshitake A., Miyamoto J., Hirose M. and Ito N. (1989). DNA-adduct formation in the forestomach of rats treated with 3-*tert*-butyl-4-hydroxyanisole and its metabolites as assessed by an enzymatic ³²P-postlabeling method. *Cancer Lett.*, 48: 189-195.
 32. Schilderman P.L., Rhijnsburger E., Zwingmann I. and Kleinjans J.C.S. (1995). Induction of oxidative DNA damage and enhancement of cell proliferation in human lymphocytes *in vitro* by butylated hydroxyanisole. *Carcinogenesis*, 16: 507-512.
 33. Schilderman P.L., van Maanen J.M.S., Smeets E.J., ten Hoor F. and Kleinjans J.C.S. (1993). Oxygen radical formation during prostaglandin H synthase-mediated biotransformation of butylated hydroxyanisole. *Carcinogenesis*, 14: 347-353.
 34. Shibata M.A., Asakawa E., Hagiwara A., Kurata Y. and Fukushima S. (1991). DNA synthesis and scanning electron microscopic lesions in renal pelvic epithelium of rats treated with bladder cancer promoters. *Toxicol. Lett.*, 55: 263-272.
 35. Tice R.R., Agurell E., Anderson D., Burlinson B., Hartmann A., Kobayashi H., Miyamae Y., Rojas E., Ryu J.C. and Sasaki Y.F. (2000). The single cell gel/comet assay: guidelines for in vitro and in vivo genetic toxicology testing. *Environ. Mol. Mutagen.*, 35: 206-221.
 36. Tu T., Giblin D. and Gross M. (2011). Structural determinant of chemical reactivity and potential health effects of quinones from natural products. *Chem. Res. Toxicol.*, 24 (9): 1527-1539.
 37. Vinken M., Doktorova T., Decroock E., Leybaert L., Vanhaecke T. and Rogiers V. (2009). Gap junctional intercellular communication as a target for liver toxicity and carcinogenicity. *Crit. Rev. Biochem. Mol. Biol.*, 44(4): 6201-6222.
 38. Visvardis E-E., Tassiou A.M. and Piperakis S.M. (1997). Study of DNA damage induction and repair capacity of fresh and cryopreserved lymphocytes exposed to H₂O₂ and γ-radiation with the alkaline comet assay. *Mutat. Res.*, 383: 71-80.
 39. Williams G. M., McQueen C.A. and Tong C. (1990). Toxicity studies of butylated hydroxyanisole and butylated hydroxytoluene. I. Genetic and cellular effects. *Food Chem. Toxicol.*, 28: 793-798.

12/31/2011

個別化医療のための バイオマーカーの探索・バリデーションと活用手法

鈴木 孝昌

国立医薬品食品衛生研究所 遺伝子細胞医薬部 室長 薬学博士

(株)技術情報協会

「個別化医療」 抜刷

第6章

個別化医療のためのバイオマーカーの 探索・バリデーションと活用手法

はじめに

個別化医療の実現に向け、個人差を判定するためのバイオマーカーの重要性は高まりつつある。その中心には、ヒトゲノム解析がもたらした資産であるヒト遺伝子多型情報の活用があげられる。酵素活性に影響を与える一塩基多型 (SNP) など、実際にその生理学的意義が確立しバイオマーカーとして実用化されて始めているものもある。また、こうした遺伝子多型を検出するためのDNAチップをはじめとする診断技術の進歩もその応用に向けて後押しをしている。DNAチップを用いた解析では、遺伝子発現情報に基づいて癌の個性診断を行うという手法も実用化され始めており、そのバリデーションも課題となっている。さらに、質量分析機器の進歩によるプロテオーム解析技術の向上により、より直接的な生体機能分子としてのタンパク質の発現動態の変化から個別医療のためのバイオマーカー検出の試みも盛んである。特にこうしたバイオマーカーは、治療のための標的分子としても有用であり、今日、分子標的治療薬の選択にあたり、その有効性の診断にも利用されている (表 1)。こうした、遺伝子、あるいはタンパク質の配列や発現量を指標とするバイオマーカーの個別化医療への応用に関して、その探索、バリデーションおよび活用手法を、レギュラトリーサイエンスという視点も踏まえて概説する。

表 1 分子標的治療薬と診断

薬剤名	対象疾患	分子標的	診断標的	診断法
イマチニブ (グリベック®)	慢性骨髄性白血病 (CML) フィラデルフィア染色体 陽性急性リンパ性白血病	bcr-abl 融合遺伝子 (フィラデルフィア染色体)	bcr-abl 融合遺伝子, フィラデルフィア染色体	PCR 核型解析 (FISH)
イマチニブ (グリベック®)	KIT (CD117) 陽性消化 管間質腫瘍 (GIST)	変異型 c-Kit	c-Kit 過剰発現 / c-kit 遺伝子変異	免疫組織化学染色 / シークエンス解析
イリノテカン (カンプト注®, トボテシン®)	肺癌, 転移性大腸癌など	トポイソメラーゼ I	UGT1A1 遺伝子	多型解析 (インベーター法)
エルロチニブ (タルセバ®)	非小細胞肺癌	上皮成長因子受容体 (EGFR) チロシンキナーゼ活性	EGFR 過剰発現	免疫組織化学染色
ゲフィニチブ (イレッサ®)	非小細胞肺癌	上皮成長因子受容体 (EGFR) チロシンキナーゼ活性	上皮細胞成長因子受容体 (EGF 受容体) 遺伝子	免疫組織化学染色
トラツズマブ (ハーセプチン®)	HER2 過剰発現転移性乳癌	HER2 蛋白	Her2 タンパク質 / Her2 遺伝子	免疫組織化学染色 / 蛍光 in situ ハイブリダイゼーション (FISH)
リツキシマブ (リツキサン®)	B 細胞性非ホジキンリンパ腫	CD20 タンパク質	CD20 タンパク質	免疫組織化学染色 フローサイトメトリー
セツキシマブ (アービタックス®)	EGFR 陽性結腸直腸癌	上皮成長因子受容体 (EGFR)	EGF 受容体タンパク質, K-ras 遺伝子	シークエンス解析, RFLP, SSCP

1. 患者選定のためのバイオマーカーとその測定方法

1.1 遺伝子多型

遺伝病に代表される生殖細胞を介した遺伝子変異は、広義には遺伝子多型であり、その頻度が異なる（一般に出現頻度として1%以上の変異を多型と呼ぶ）だけなので、同列に扱うことができ、検出方法も同一となる。一方、後天的な変異、例えば癌細胞における癌関連遺伝子の変異は、一部遺伝性の変化もあるが、大部分は体細胞において、複製エラーや様々な発癌物質等の環境因子によって引き起こされた後天的な突然変異が引き金となり、遺伝子多型とは異なるものである。この場合、一部の細胞が他とは異なる配列を持つことになり、検出もその分難しくなる。LCMなど癌細胞をなるべく純化して取り出す技術との組み合わせも要求される。

遺伝子多型に関しては、SNPに加えて最近ではコピー数の変化（CNV）がその測定技術の進歩とともに個人の差を規定する因子として重要であることがわかってきている¹⁾。ある種の精神疾患や癌とも密接にかかわっていることが知られており、今後遺伝子診断の分野においても重要な位置を占めると考えられる。

さらに、特定の遺伝子多型（変異）の検出法としては、現在もDNAシーケンサーによる直接シーケンス法が行われているが、次世代、次々世代のハイスループットなシーケンサーの登場により、シーケンス解析のコストが大幅に下がることが期待され²⁾、全ゲノム解析が俗に言う\$1000で達成できるようになれば、診断に際してもとりあえず全ゲノムの情報を解析するというような時代が、近い将来にやってくることも十分予想できる。そうなれば、遺伝子の多様性と疾病、薬剤反応性の個人差との関連に関して、今後いっそう理解が深まることが期待される。

1.2 染色体レベルでの変化

遺伝子配列レベルでのミクロな変化に対し、マクロな変化である染色体レベルでの構造変化は、古くから染色体を顕微鏡下で直接観察することにより異常を検出してきた。ダウン症における21番染色体トリソミーや慢性骨髄性白血病におけるフィラデルフィア染色体のように、光学顕微鏡を用いた染色体観察により診断がつく例も多いが、最近ではPCRを用いた融合遺伝子の増幅や蛍光in situハイブリダイゼーション法（FISH）などの分子生物学的な手法に置き換わりつつある。即ち、検査行為が“製品”としての診断薬に置き換えられ、誰でもが行える検査となっており、特に、従来光学顕微鏡では観察が不可能であった微細な染色体変化や染色体転座などの検出には、有効な手段となっている。こうした例として、ゲノムワイドに染色体の増減の変化を調べるComparative Genome Hybridization（CGH）技術が注目される³⁾。当初は染色体標本を用いて蛍光顕微鏡による観察により行われてきたが、近年、マイクロアレイを用いる方法（ア

レイ CGH) が開発され、解析精度が飛躍的に進歩した。遺伝子多型の解析と合わせ、ゲノムワイドな個人の感受性診断という観点から、今後臨床応用が期待される分野である。

1.3 遺伝子発現解析

遺伝子配列情報の解読と、微小領域に高密度に核酸を固定化する技術の組み合わせにより、マイクロアレイや DNA チップといった遺伝子発現を網羅的に解析可能な革新的なツールが開発された。前述の SNP 等の遺伝子型を調べる目的としても使用されているが、遺伝子の発現量の変化を網羅的に調べるという本来の用途としても、臨床応用が期待される。DNA チップ (マイクロアレイ) は、その網羅性という点が最大の特長であり、複数の遺伝子の発現情報を組み合わせることにより一つの診断結果を導くという、従来とは全く違ったアプローチを取る。FDA では、こうした新しいタイプの診断法を *in vitro diagnostic multivariate index assay (IVDMIA)* というカテゴリーのひとつとして捉え、2006 年に IVDMIA Draft Guidance を公表している⁴⁾。DNA チップ等による発現解析は、どのような遺伝子の発現が目的とする疾患の診断に有用であるかを、開発の段階で網羅的な遺伝子発現情報を元に絞り込んでいくもので、通常、絞り込みが行われた遺伝子セットの情報をもとに、一定のアルゴリズムを用いて目的とする診断結果を導くことになる。必要となる遺伝子数が比較的多い場合には、同じプラットフォームを用いたフォーカスチップ (アレイ) という形で実際の診断ツールが提供されるが、遺伝子数が数十以下と絞り込まれてきた場合には、より信頼性の高い手法として、定量的リアルタイム PCR (qPCR) 法を用いて検出するアプローチも取られる。すでに研究用としては各種リアルタイム PCR 機器が普及しており、カード型のアレイにマルチプレックスに複数遺伝子の qPCR 解析が可能なツール (TaqMan® Array Cards) も開発されている⁵⁾。

1.4 タンパク質バイオマーカー

従来バイオマーカー分子としては、肝機能検査における血液中の酵素や酵素組織免疫化学法のようにタンパク質を標的とするものが多かった。これに対し、ゲノム解析技術の進展により、遺伝子型およびその発現が新たなバイオマーカーとして台頭してきたわけであるが、その産物であるタンパク質も派生的に新しいバイオマーカーとして注目されている。そこに近年の質量分析技術の進歩によるプロテオーム解析技術が普及したことが背景となり、直接的にタンパク質あるいはペプチドを標的としてバイオマーカーの探索を行うアプローチが盛んとなってきた⁶⁾。遺伝子発現解析と比べるとプロテオーム解析は網羅性と感度の点でまだ劣っているが、リン酸化や糖鎖などの翻訳後修飾を解析することができ、生体機能分子を直接マーカーとして検出できる点で魅力がある。検出したバイオマーカーは、その抗体を作成することにより従来の ELISA 法等を

用いた簡便な診断法へと移行できる。さらに、MS/MS 測定を利用して、抗体を作成しなくても質量分析計で直接目的タンパク質を検出、定量可能とする選択的イオンモニタリング (Selected Reaction Monitoring) およびそれを複数組み合わせる Multiple Reaction Monitoring の手法が将来 ELISA 法に変わりうる技術として注目されている⁷⁾。最近では、完全長 cDNA を使ってすべてのタンパク質を合成し、質量分析装置で解析することにより、各タンパク質に特異的な MS および MS/MS シグナルペアを網羅的に抽出し、すべてのタンパク質に対して特異的 SRM を設定することにより、高感度に全タンパク質の定量を可能にする試みも始まっている⁶⁾。

1.5 その他のバイオマーカー

その他のバイオマーカーとして最近注目されているものに、エピジェネティクスがあげられる。ゲノムの配列情報の一部であるため遺伝子多型に近いが、多型が先天的なものであるのに対し、こちらは後天的、動的な変化であり、組織や細胞レベルでも変化するためその測定はより難しいものとなる。分子レベルでは、DNA のメチル化 (CpG アイランドの C のメチル化による 5 メチルシトシン) の有無を、目的遺伝子およびゲノムワイドに検出する。エピジェネティクスの本体である遺伝子のメチル化の変化は、その近傍の遺伝子の発現の変化として現れるため、2 次的には遺伝子発現解析によっても検出できることになるが、検出手法としてはより簡便でわかりやすい結果を導くものとして期待される。最近では、各種がん細胞において、がん関連遺伝子のメチル化の変化が報告されており、臨床的エビデンスが蓄積されつつある⁸⁾。また、癌以外の疾患でも、統合失調症における reelin 遺伝子のメチル化や、自閉症、糖尿病など様々な疾患でエピジェネティクスの関与が示唆されている。検出手法に関しては、既に Bisulfite sequencing 法、クロマチン免疫沈降法などの手法が用いられているが、今後臨床診断へと応用するにあたっては、さらに効率的な手法や解析機器の開発が鍵となるであろう。

次に、プロテオームに続くオミックス解析として注目されるメタボローム解析によってもたらされる低分子代謝産物が、新たなバイオマーカーとして開発される可能性も高い⁹⁾。もともと、古典的には血糖値や尿酸値といったものが診断に利用されてきたわけであるので、こうしたカテゴリーに入る新規のバイオマーカーは診断薬としてもなじみやすい。例として、代謝性疾患における特定代謝産物の増加などが挙げられるが、異常までいかないレベルであっても、代謝能の変化が個人の薬物感受性に寄与することはファーマコゲノミクスの観点からも明らかであり、今後は遺伝子ではなく直接代謝産物の側からバイオマーカーの開発を行うというアプローチも増えるであろう。この領域においても、プロテオームと同様、質量分析機器の果たす役割は大きい。

さらに今後注目される分野として、分子イメージングによるバイオマーカーの検出があげられる。PET や MRI といった臨床イメージング技術の進歩により、これまでは直接観察できな

かったバイオマーカーの動態を、生体を用いてリアルタイムで検出ができるようになってきている¹⁰⁾。こうした技術とバイオマーカーを組み合わせた生体イメージングにより非侵襲的な病理診断や治療効果の判定などに役立つ新たな診断法が開発されることが期待される。

2. バイオマーカーの診断利用の実例

2.1 遺伝子多型

もっとも臨床応用が進んでいるのが、薬物代謝酵素の多型である。遺伝子配列変化やコピー数変化により酵素活性が変化することにより、関与する薬剤の薬物動態が変化し、効果や副作用に個人差が見られる原因となる。薬物代謝酵素の多型として一番身近な例は、アルコール代謝能に及ぼすアセトアルデヒド脱水素酵素 (ALDH) の多型であり、変異型アレルをヘテロおよびホモに持つことにより、アルコールに対する感受性が変化し、お酒に弱いまたは全く飲めない体質となる。代謝酵素の多型については、DNA チップを用いて複数の遺伝子多型を同時に検出するロッシュダイアグノスティック社の AmpliChip CYP450 が国内で体外診断薬としての認可を受け、市販されている¹¹⁾。これは、表 2 に示すように CYP 2C19、および CYP 2D6 の複数の多型を検出し、薬剤の感受性を予測するものである。注意すべきは、遺伝子型の診断薬としての有効性はあくまで遺伝子型を正しく判定できるかどうかという点にあり、関連性が予想される薬剤への感受性を判断するものではないという点である。遺伝子多型と薬剤の代謝に関しては別途臨床的なエビデンスの蓄積が重要であり、それらを総合して治療の判断を行わなければいけない。もちろん、遺伝子型だけですべてが決まるわけではなく、未知の多型などその他の要因によって薬物代謝

表 2 AmpliChip® CYP450 が検出できる多型と関連する薬剤

CYP 分子種	検出できる多型	薬物代謝能の判定	関連薬剤
CYP 2D6	27 種類 (1, 2ABD, 3, 4ABDJ, 5, 6ABC, 7, 8, 9, 10AB, 11, 15, 17, 19, 20, 29, 35, 36, 40, 41, 1XN, 2XN, 4XN, 10XN, 17XN, 35XN, 41XN)	E: 一般的 (Extensive metaboliser) I: 低い (Intermediate metaboliser) P: 著しく低い (Poor metaboliser) U: 高い (Ultra-rapid metaboliser)	ベータ遮断薬 Carvedilol, Metoprolol など 抗うつ薬 Imipramine, Amitriptyline など 抗精神薬 Haloperidol, Thioridazine など その他 Codeine, Tamoxifen など
CYP 2C19	3 種類 (1, 2, 3)	E: 一般的 (Extensive metaboliser) P: 著しく低い (Poor metaboliser)	プロトンポンプ阻害薬 Omeprazole, Lansoprazol など 抗てんかん薬 Diazepam, Phenytoin など その他 Cyclophosphamide, Progesterone など

能に影響を受ける可能性もあることから、従来の臨床薬物動態解析の重要性は変わらない。

また、イレッサにおける UGT1A1 遺伝子多型のインベーター法による検出¹²⁾ など、多型の検出技術や解析装置の開発も進み、今後ますます臨床応用される例も増えることが予想される。

2.2 遺伝子発現解析

癌遺伝子の過剰発現など、遺伝子発現がバイオマーカーとなりうるケースも多いが、実際には原因となる遺伝子異常の検出や発現しているタンパク質を免疫染色により検出する場合が多く、遺伝子発現をバイオマーカーとして利用する際には、DNA チップに代表されるように複数の遺伝子発現情報を元に診断を行うケースが中心となる。国内ではまだ遺伝子発現解析に基づく DNA チップ等の新しい診断法として承認された例はないが、海外では既に承認を受けて臨床応用されている例もある。

DNA マイクロアレイを用いた遺伝子発現解析による診断法としては、欧米ではオランダの Agendia 社が開発した MammaPrint[®] が、2005-7 年にかけて体外診断薬としての認可を初めて取得した。MammaPrint[®] は 70 遺伝子の発現情報をもとに、乳癌の予後予測を行うもので、治療法の選択に有益な情報を与える。遺伝子発現解析に基づく体外診断薬として FDA が承認しているものとしては、MammaPrint[®] の他にも、心臓移植後の拒絶反応を予測する XDx 社の AlloMap[®] (qPCR) および Pathwork Diagnostic 社の Pathwork[®] Tissue of Origin (DNA Chip) があり、それぞれ図 1 に示す特徴を持っている。また、これら承認を受けた以外にも、様々な製品が Laboratory Developed Test (LDT) として使われている。その代表例が MammaPrint[®] と同様に乳癌の予後予測に用いられる OncotypeDX[®] であり、臨床的にはむしろこちらの方が米国では普及している¹³⁾。FDA の認可は得ていないが、Clinical Laboratory Improvement Amendments (CLIA) によって認証を受けた機関で検査される LDT として保険も適応されてい

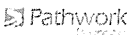

FDA に認可された IVD/MIA	
・ MammaPrint [®] (2007 年 2 月) — Agilent microarray (70 遺伝子) — 乳癌の遠隔転移 (予後) 予測	
・ Pathwork [®] Tissue of Origin (2008 年 7 月) — Affymetrix PathChip (1550 遺伝子) — 15 種類の典型的な癌のタイプを分類	
・ AlloMap [®] Molecular Expression Testing (2008 年 8 月) — リアルタイム PCR (11 + 9 control 遺伝子) — 心臓移植の拒絶の予測	

図 1